Supporting Information

On the Role of Plasmonic $Ti_3C_2T_x$ MXene in Enhancing Photoredox Catalysis

Guanshun Xie[a], Chuang Han[b], Fei Song[a], Yisong Zhu[a], Xuanyu Wang[a], Jialin Wang[a], Zhenjun Wu[c], Xiuqiang Xie[a,], Nan Zhang[a,*]*

Contents list

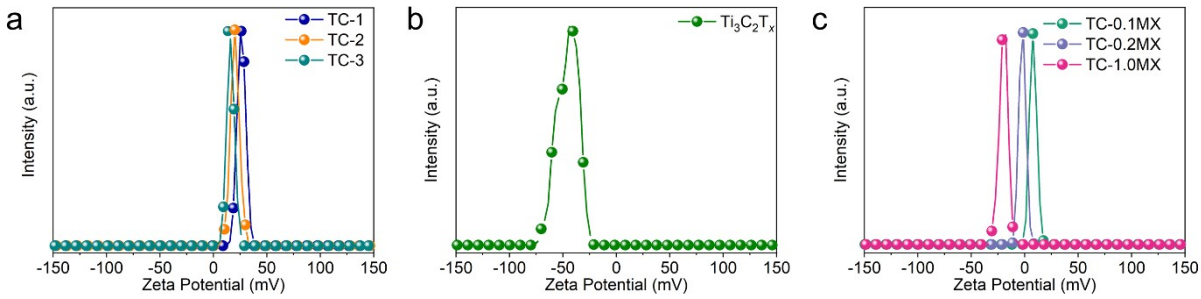

Figure S1. Zeta potentials of the as-prepared samples.

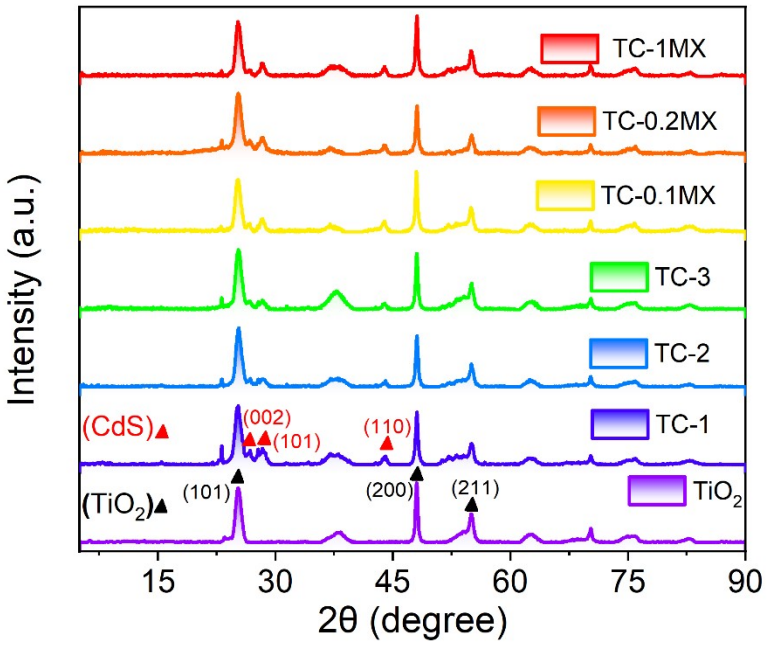

Figure S2. XRD patterns of TiO_2, TC, and TC-MX composites.

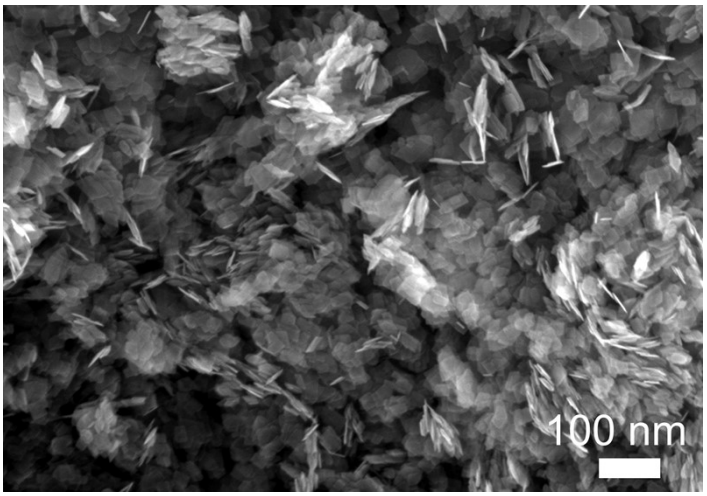

Figure S3. SEM image of TiO_2 nanosheets.

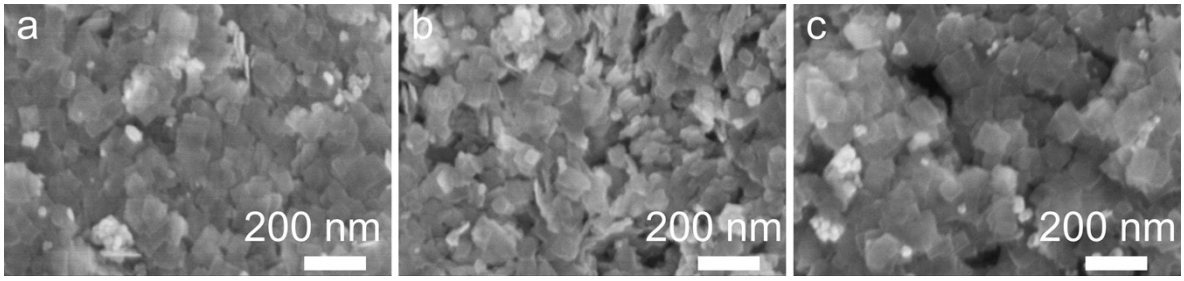

Figure S4. SEM images of (a) TC-1, (b) TC-2, and (c) TC-3.

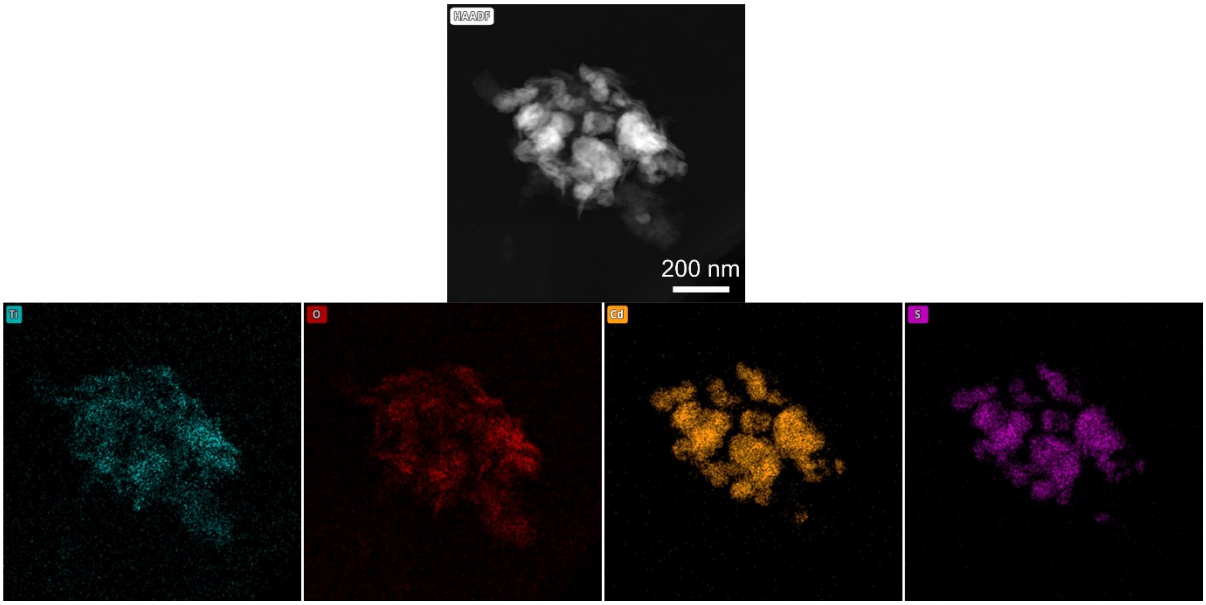

Figure S5. HAADF-STEM image of TC-2 with the corresponding Ti, O, Cd, and S EDX mapping results.

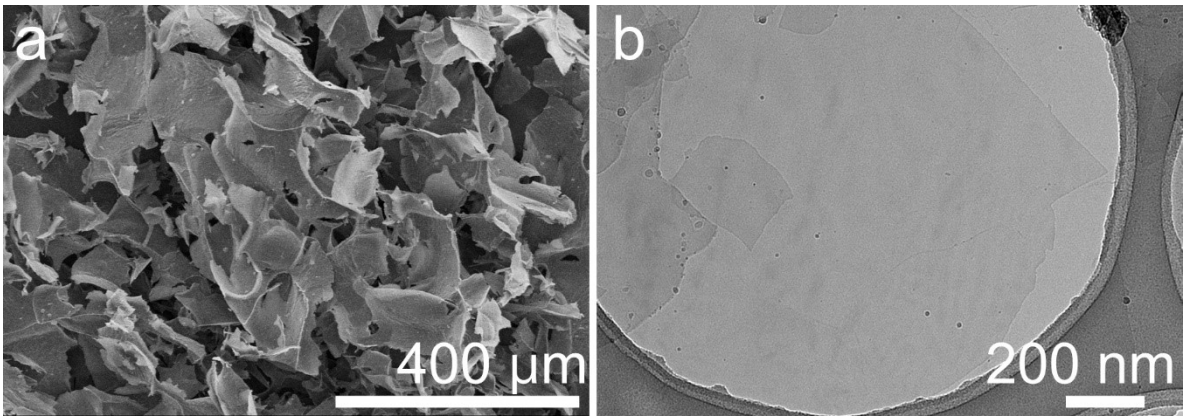

Figure S6. (a) SEM and (b) TEM images of $Ti_3C_2T_x$.

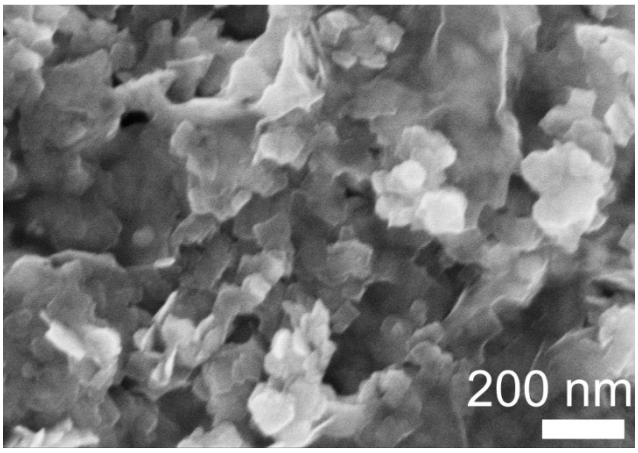

Figure S7. SEM image of TC-0.1MX.

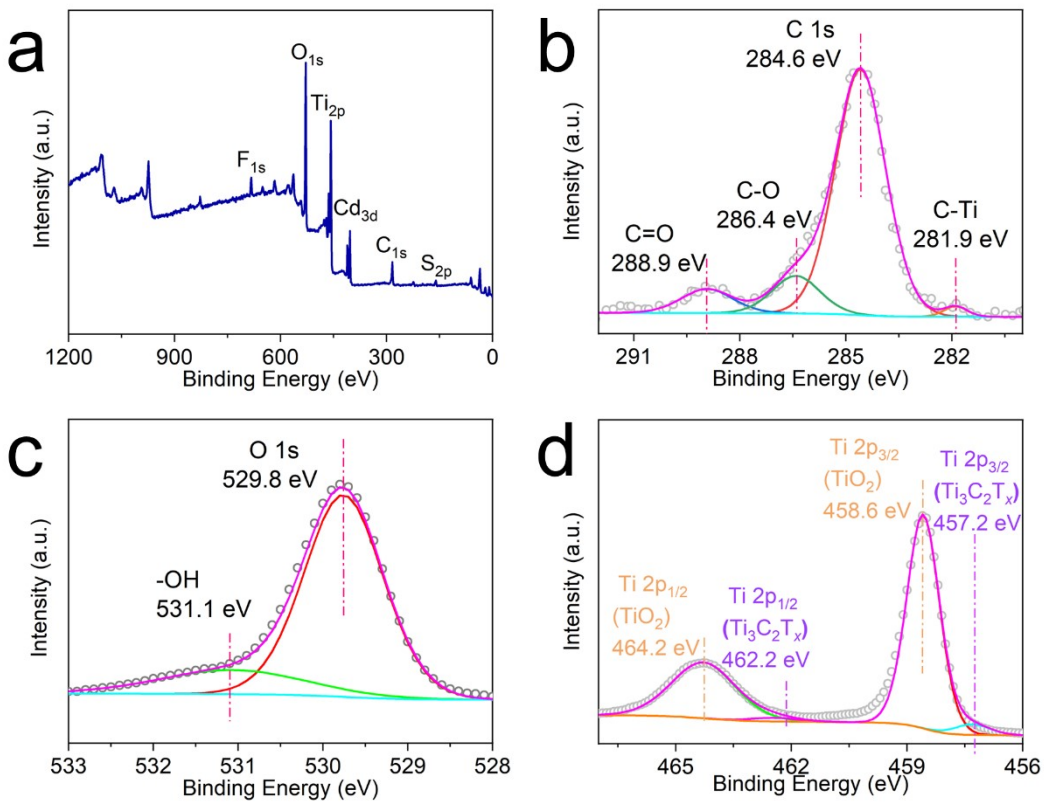

Figure S8. XPS spectrum of TC-0.1MX: (a) Survey, (b) C 1s, (c) O 1s and (d) Ti 2p.

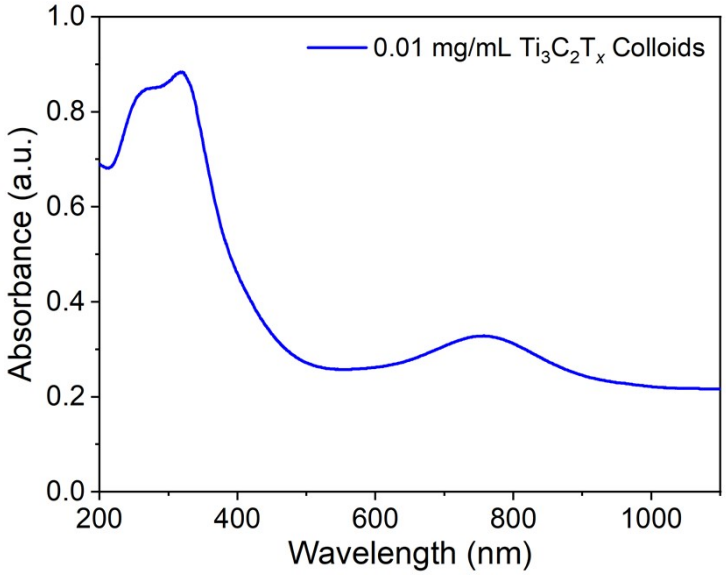

Figure S9. Ultraviolet-visible-NIR light absorption spectrum of $Ti_3C_2T_x$ colloid.

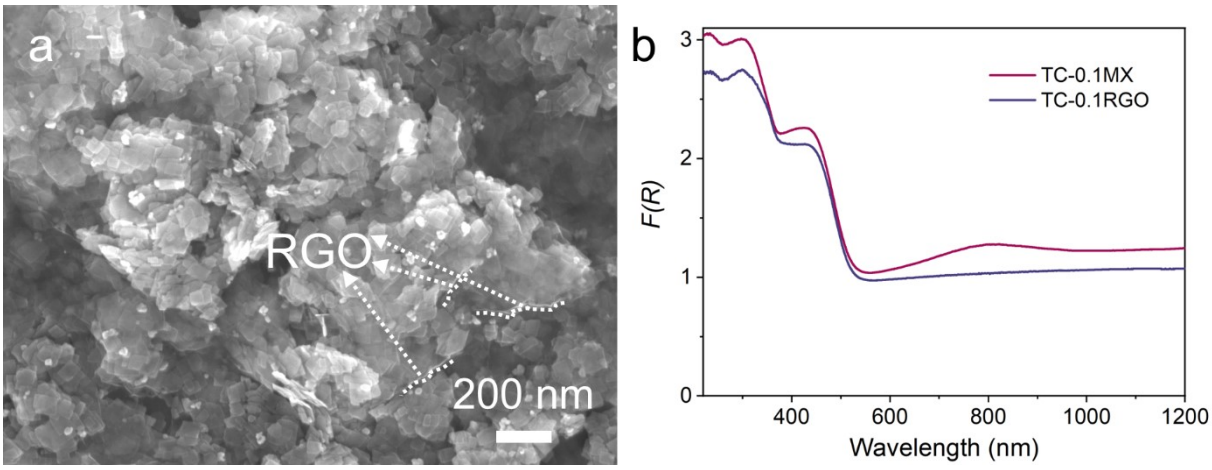

Figure S10. (a) SEM image of TC-0.1RGO. (b) UV-vis diffuse reflectance spectra (DRS) of TC-0.1MX and TC-0.1RGO composites.

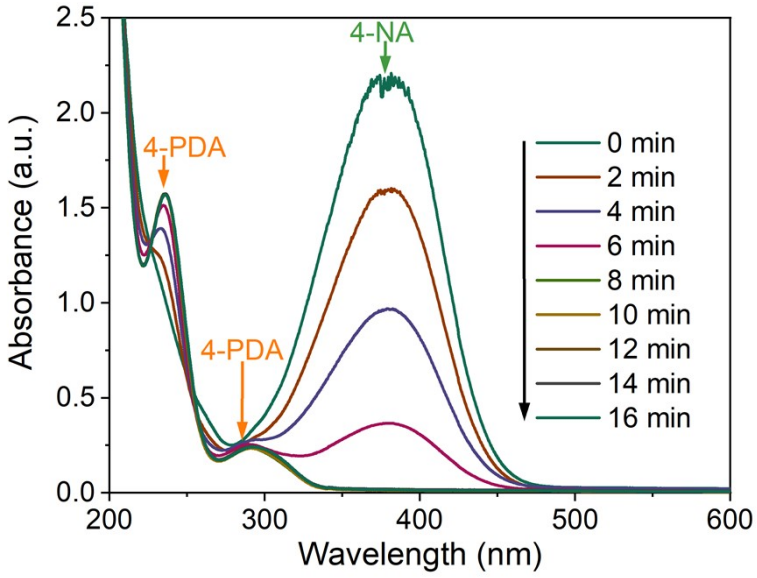

Figure S11. UV−vis absorption spectra of 4-NA aqueous solution over TC-0.1MX nanocomposite under visible light irradiation (λ > 420 nm) with the addition of ammonium formate as quencher for photogenerated holes under N_2 purge.

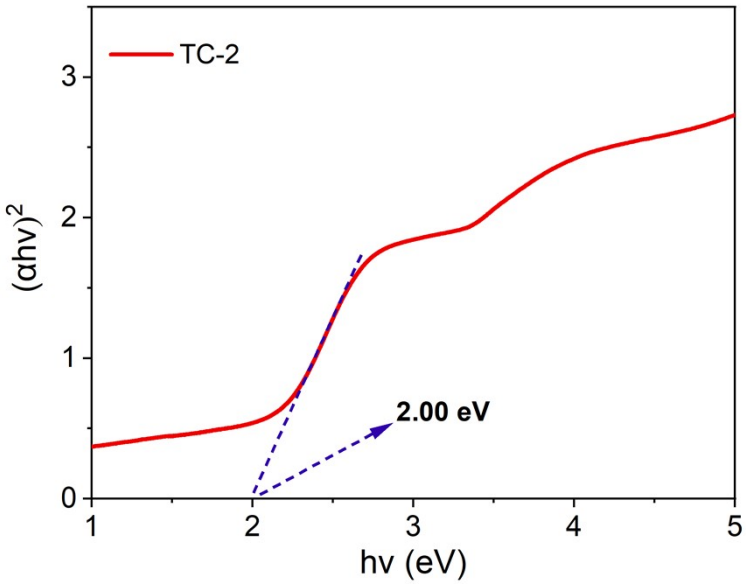

Figure S12. Transformed plots based on the Kubelka–Munk function versus photon energy for TC-2.

Note: As TiO_2 has no light absorption in the visible region of TiO_2@CdS (**Figure 2c**), the E_g obtained corresponds to CdS.

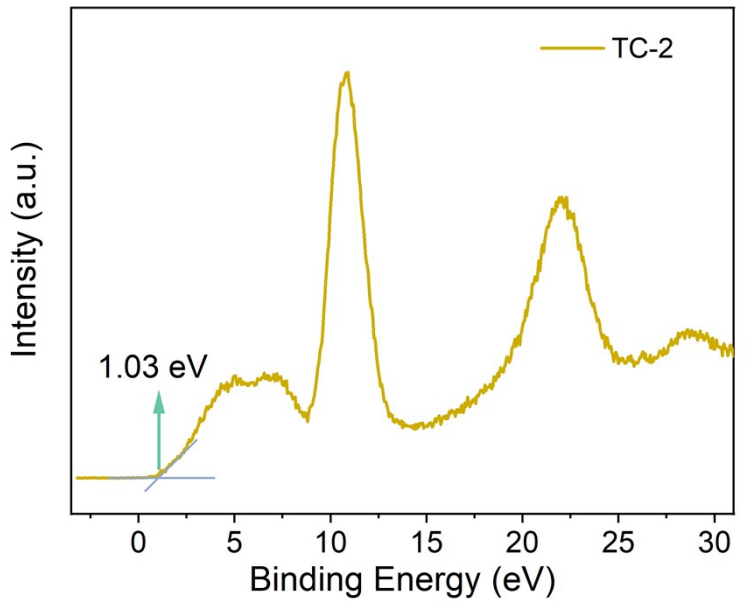

Figure S13. XPS valence band spectrum of TC-2.

Note: The valence band energy (E_{VB}) of TiO_2@CdS composite is attributed to CdS by XPS, because CdS is coated on the surface of CdS and the XPS detection depth is only ~5 nm.

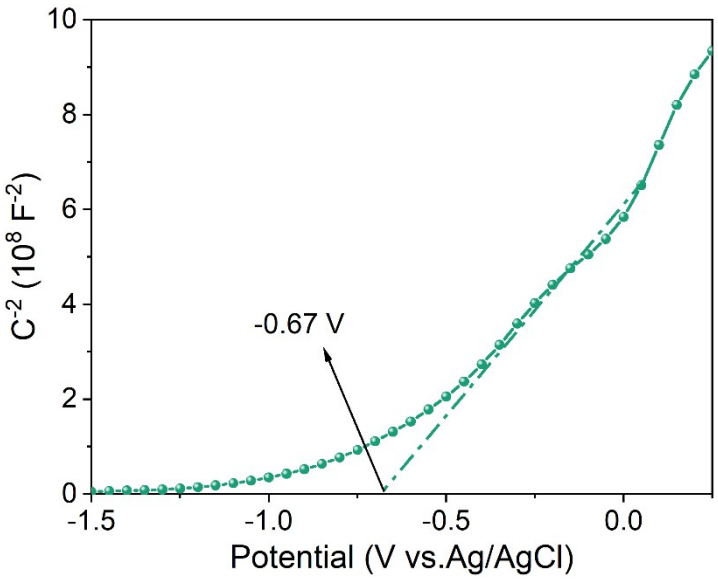

Figure S14. Mott-Schottky plots of TiO_2.

Note: It is seen from **Figure S14** that the flat-band potential of TiO_2 is estimated to be around −0.67 V versus Ag/AgCl (pH = 6.8, for 0.2 M Na_2SO_4 electrolyte). It is known that the bottom of conduction band in n-type semiconductors is more negative by about −0.2 V than the flat band potential[1]. The conduction band of TiO_2 is calculated to be −0.27 V versus normal hydrogen electrode (NHE, pH = 0)[2].

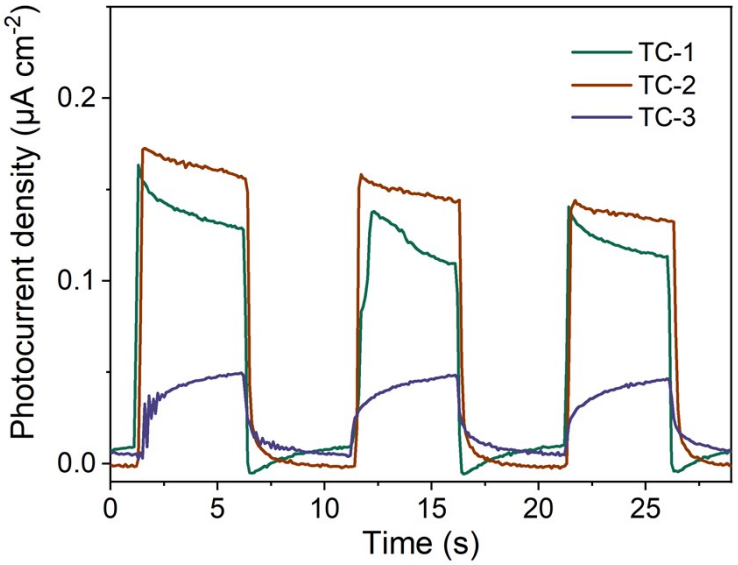

Figure S15. Photocurrent densities of TC-1, TC-2, and TC-3 under visible-NIR light irradiation (λ > 420 nm).

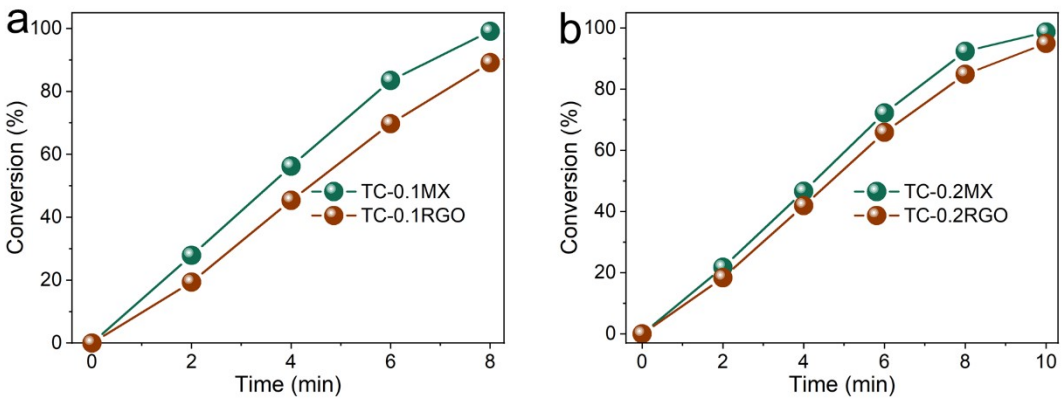

Figure S16. Photoactivities of TC-0.1RGO a) and TC-0.2RGO b) composites for the selective reduction of 4-nitroaniline (4-NA) to 4-phenylenediamine (4-PDA) in water with the addition of ammonium formate as a hole scavenger and N_2 purging in water under visible-NIR light irradiation ($\lambda > 420$ nm).

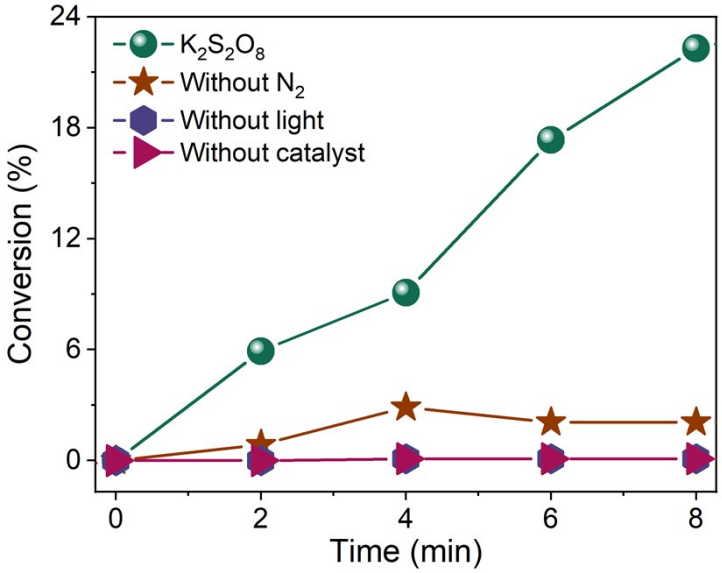

Figure S17. Control experiments for photocatalytic reduction of 4-NA over TC-0.1MX: reaction with $K_2S_2O_8$ as a scavenger for electrons, and reaction without the purge of N_2, without light, without catalyst.

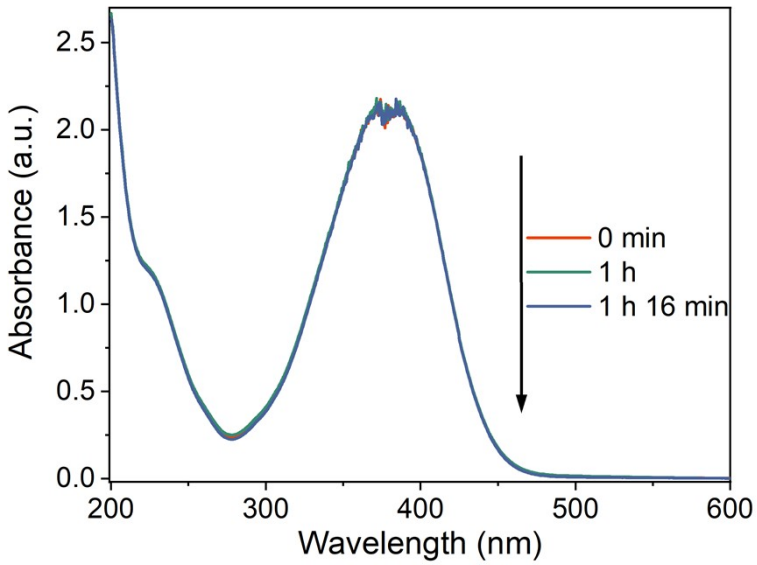

Figure S18. UV-vis absorption spectra of 4-NA over TC-0.1MX under adsorption equilibrium.

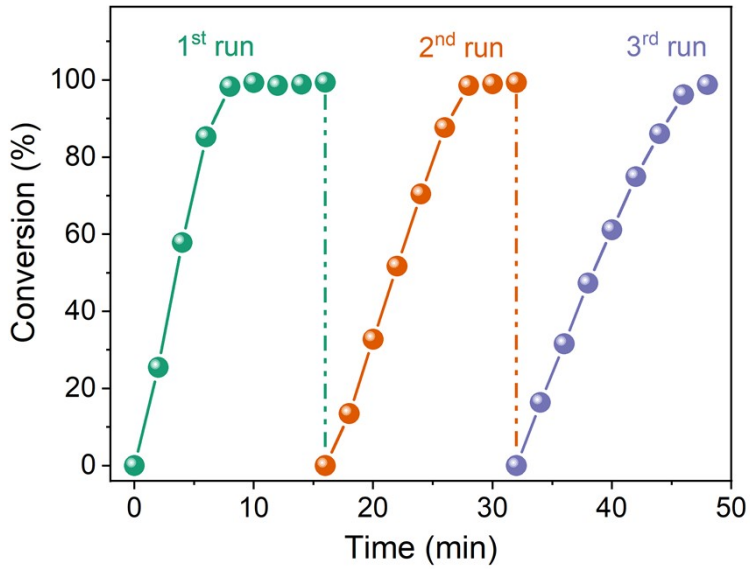

Figure S19. Stability test of TC-0.1MX.

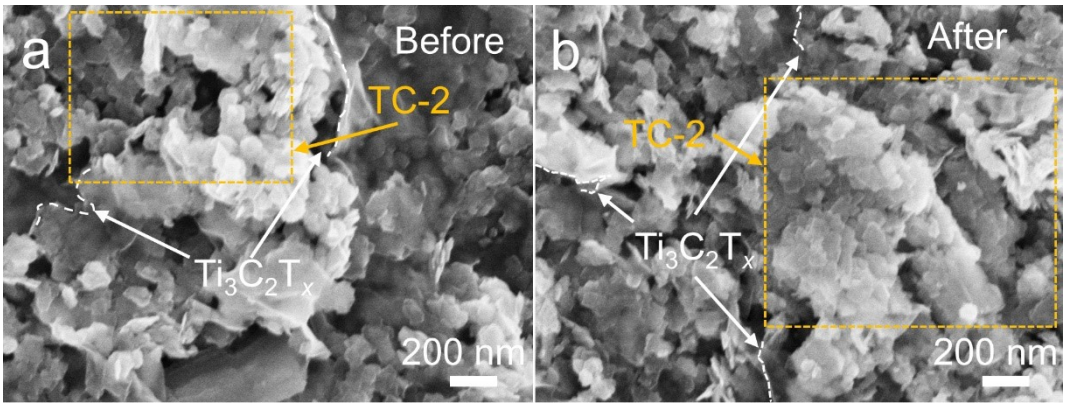

Figure S20. SEM images of (a) the original TC-0.1MX sample, and the TC-0.1MX sample after (b) three-cycle photocatalysis reactions.

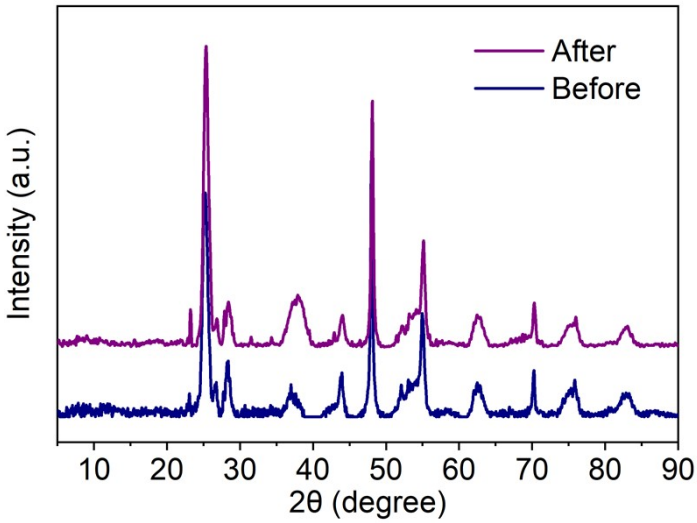

Figure S21. XRD patterns of the TC-0.1MX sample before and after three-cycle photocatalysis reactions.

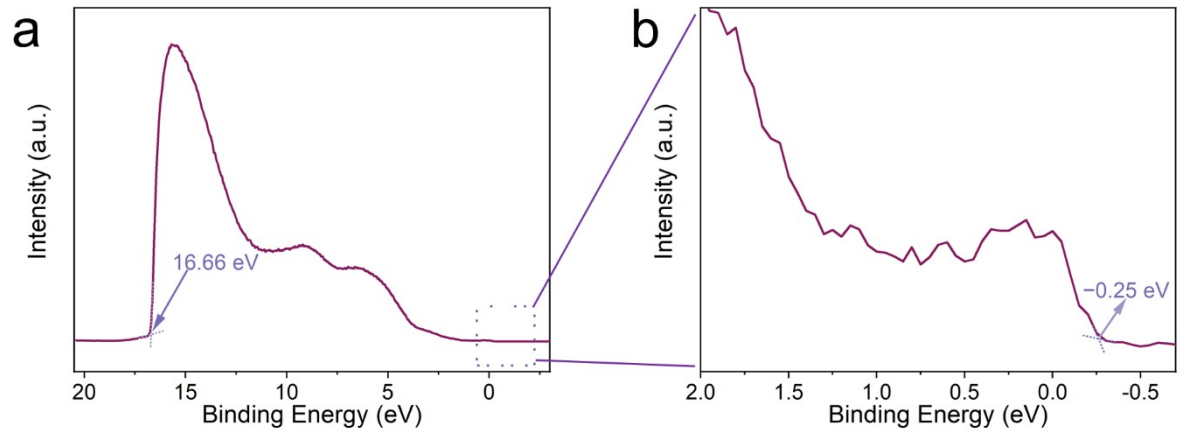

Figure S22. Ultraviolet photoelectron spectra (UPS) of the synthesized $Ti_3C_2T_x$ MXene.

Note: The excitation source was He I ($h\nu$ = 21.22 eV) and a negative bias of –9.8 eV was applied during the UPS measurement. The following formula is used to calculate the work function (Φ) of $Ti_3C_2T_x$:

$$\Phi = h\nu - W = 21.22 - 16.91 = 4.31 \text{ eV}$$

where W is the width of the UPS spectrum. Then, the Fermi level (E_F) of $Ti_3C_2T_x$ is calculated as follows[3]:

$$E_F = E_{vac} - \Phi$$

where E_{vac} is the energy of a stationary electron at vacuum level (assumed as 0 eV). Therefore, it can be estimated that the E_F of the $Ti_3C_2T_x$ is located at −4.31 eV vs. vacuum level. According to the relationship between the Evac and the normal electrode potential (E_{NHE}), $E_{vac} = -E_{NHE} - 4.44$[3], the E_F of $Ti_3C_2T_x$ is thus determined to be −0.13 V vs. normal hydrogen electrode.

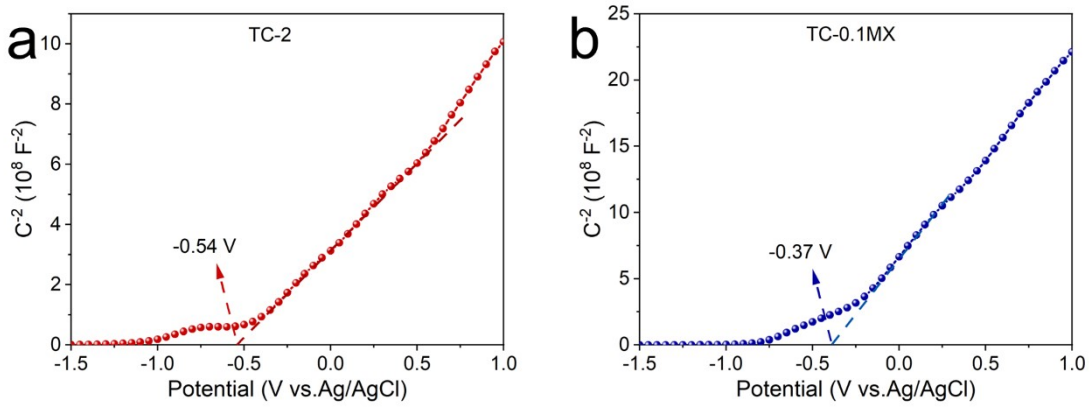

Figure S23. Mott-Schottky plots of TC-2 and TC-0.1MX.

Note: The flat band potential is obtained from the Mott-Schottky curve corresponding to the apparent Fermi level after the Fermi-level equilibration of the different components.

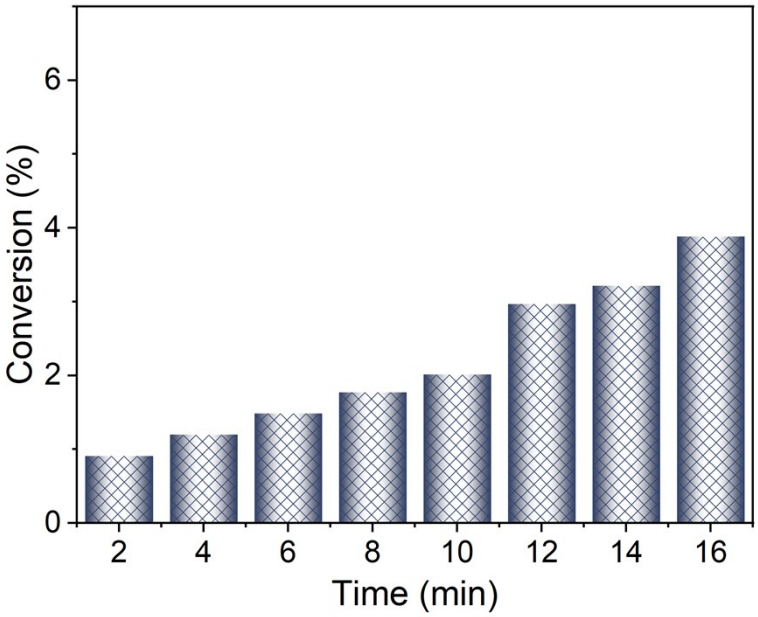

Figure S24. Photoactivities of TC-0.1MX for selective reduction of 4-NA under light irradiation (λ > 780 nm) at room temperature.

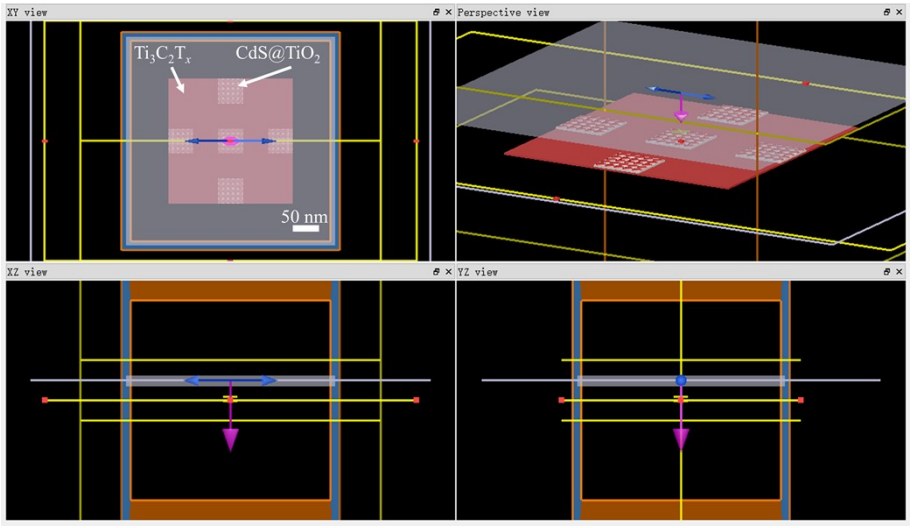

Figure S25. The finite-difference time-domain (FDTD) model consisting of CdS deposited to TiO_2 and then loaded to $Ti_3C_2T_x$.

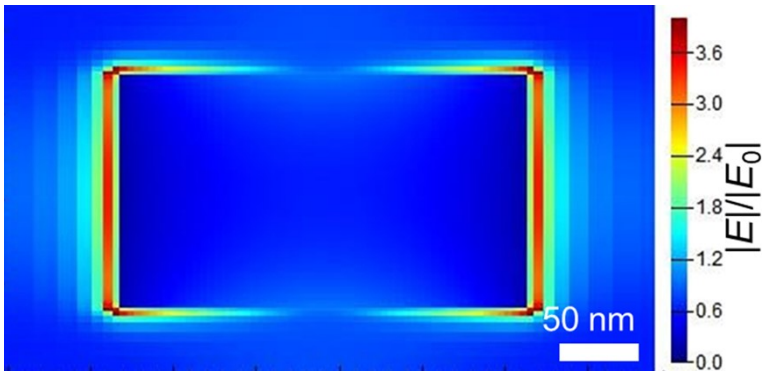

Figure S26. FDTD simulation of the near-field distributions of $Ti_3C_2T_x$.

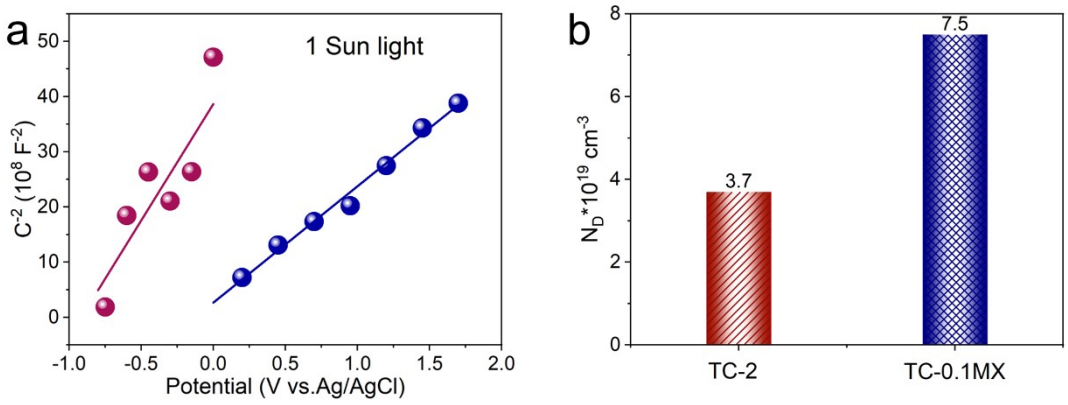

Figure S27. (a) Mott-Schottky plots for TC-2 and TC-0.1MX composites under 1 sun irradiation and (b) corresponding calculated results of the photo-induced carrier concentration.

Note: As shown in **Figure S27**, the slope of C^{-2} vs. V in the Mott-Schottky plot of TC-0.1MX decreases as compared to that of TC-2, indicating the increase of charge carriers density. The charge carriers density (N_D) is calculated to be 3.7×10^{19} and 7.5×10^{19} cm^{-3} for TC-2 and TC-0.1MX, respectively, according to the following equation[4].

$$N_D = \frac{2}{e\varepsilon\varepsilon_0}\left(\frac{d(1/C^2)}{dV}\right)^{-1}$$

where e is the elementary electronic charge, ε is the dielectric constant (8.99 for CdS[5]), ε_0 is the permittivity in vacuum, C is the capacitance, and V is the applied potential.

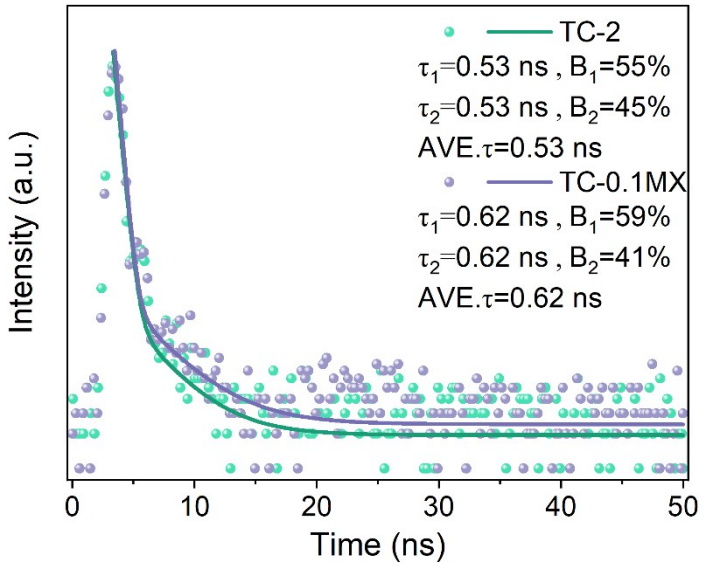

Figure S28. Time-resolved PL decay of TC-2 and TC-0.1MX.

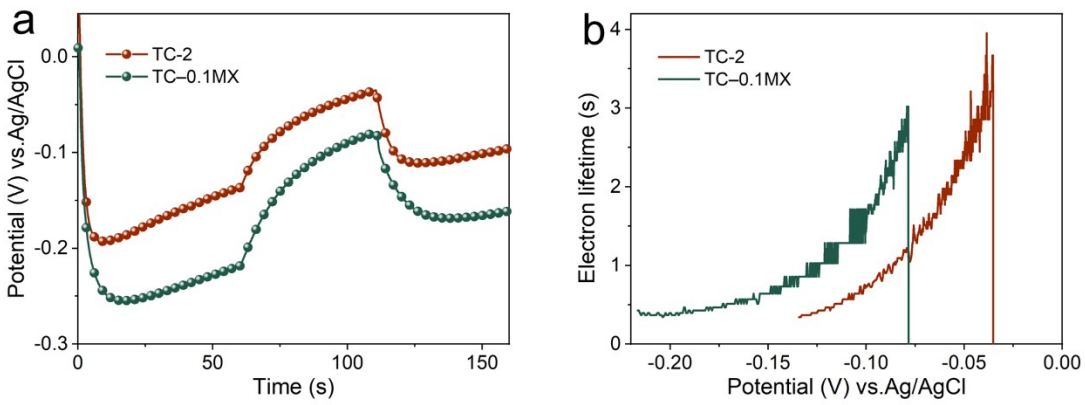

Figure S29. (a) Decay curves of photovoltage, and (b) electron lifetime of TC-2 and TC-MX composites.

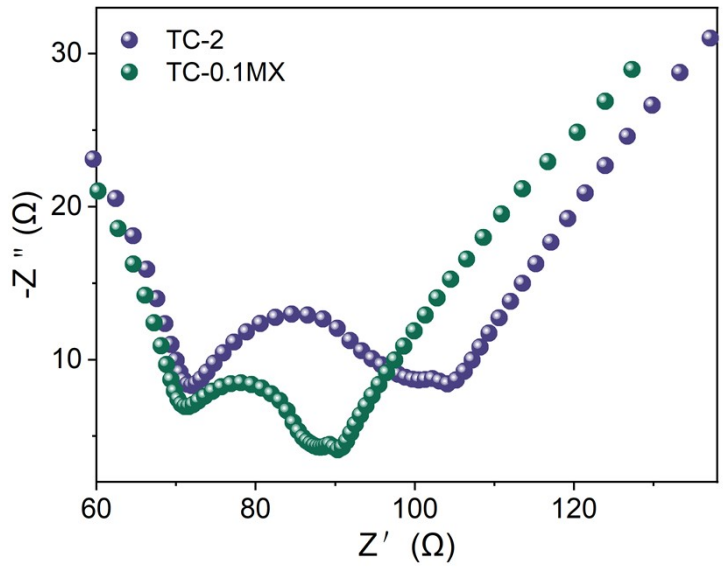

Figure S30. EIS Nyquist plots of the samples.

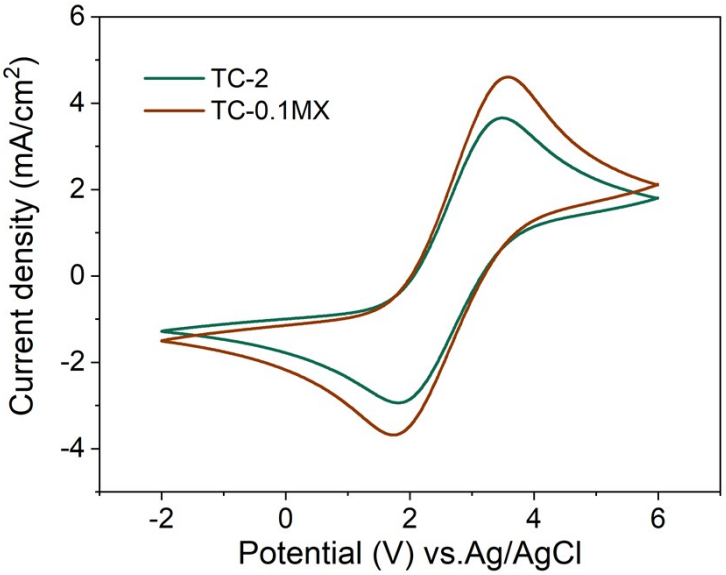

Figure S31. Cyclic voltammetry curves of TC-2 and TC-0.1MX composites at different scan rates.

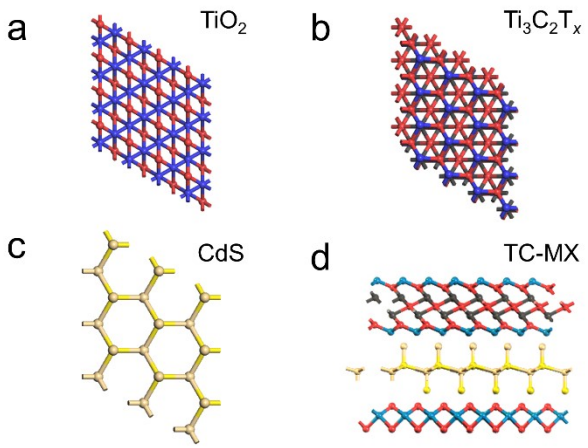

Figure S32. The top view of optimized calculation models of (a) TiO_2, (b) CdS, (c) $Ti_3C_2T_x$ and (d) TC-MX.

Table S1. XRD intensities of TiO_2 (224) and CdS (110) for different TC composites

Entry	TC-1	TC-2	TC-3
TiO_2 (224)	266	260	235
CdS (110)	545	460	344
Ratio of TiO_2 (224) to CdS (110)	0.49	0.57	0.68

References

[1] Y. Matsumoto, *J. Solid State Chem.* **1996**, *126*, 227.

[2] Y. Xu, M. A. A. Schoonen, *Am. Mineral.* **2000**, *85*, 543.

[3] J. Y. Li, Y. H. Li, F. Zhang, Z. R. Tang, Y. J. Xu, *Appl. Catal. B: Environ.* **2020**, *269*, 118783.

[4] Z. Xu, Y. Lin, M. Yin, H. Zhang, C. Cheng, L. Lu, X. Xue, H. J. Fan, X. Chen, D. Li, *Adv. Mater. Interfaces* **2015**, *2*, 1500169.

[5] C. Han, Z. R. Tang, J. Liu, S. Jin, Y. J. Xu, *Chem. Sci.* **2019**, *10*, 3514.